SCIENCE AND TECHNOLOGY ORGANIZATION
CENTRE FOR MARITIME RESEARCH AND EXPERIMENTATION

Reprint Series **CMRE-PR-2014-002**

Oceanographic field estimates from remote sensing and glider fleets

Alberto Alvarez, Baptiste Mourre

January 2014

Originally published in:

Journal of Atmospheric and Oceanic Technology, Vol. 29, 2012, pp. 1657-1662.

About CMRE

The Centre for Maritime Research and Experimentation (CMRE) is a world-class NATO scientific research and experimentation facility located in La Spezia, Italy.

The CMRE was established by the North Atlantic Council on 1 July 2012 as part of the NATO Science & Technology Organization. The CMRE and its predecessors have served NATO for over 50 years as the SACLANT Anti-Submarine Warfare Centre, SACLANT Undersea Research Centre, NATO Undersea Research Centre (NURC) and now as part of the Science & Technology Organization.

CMRE conducts state-of-the-art scientific research and experimentation ranging from concept development to prototype demonstration in an operational environment and has produced leaders in ocean science, modelling and simulation, acoustics and other disciplines, as well as producing critical results and understanding that have been built into the operational concepts of NATO and the nations.

CMRE conducts hands-on scientific and engineering research for the direct benefit of its NATO Customers. It operates two research vessels that enable science and technology solutions to be explored and exploited at sea. The largest of these vessels, the NRV Alliance, is a global class vessel that is acoustically extremely quiet.

CMRE is a leading example of enabling nations to work more effectively and efficiently together by prioritizing national needs, focusing on research and technology challenges, both in and out of the maritime environment, through the collective Power of its world-class scientists, engineers, and specialized laboratories in collaboration with the many partners in and out of the scientific domain.

NOTE: The CMRE Reprint series reprints papers and articles published by CMRE authors in the open literature as an effort to widely disseminate CMRE products. Users are encouraged to cite the original article where possible.

Oceanographic Field Estimates from Remote Sensing and Glider Fleets

A. ALVAREZ AND B. MOURRE

NATO Undersea Research Center, La Spezia, Italy

(Manuscript received 20 January 2012, in final form 26 April 2012)

ABSTRACT

This work investigates the merging of temperature observations from a glider fleet and remote sensing, based on a field experiment conducted in an extended coastal region offshore La Spezia, Italy, in August 2010. Functional optimal interpolation and spline formalisms are used to integrate temperature profiles from a fleet of three gliders with remotely sensed sea surface temperature into a volumetric thermal field estimate. Independent measurements from a towed ScanFish vehicle are used for validation. Results indicate that the optimal interpolation approach performs better than the spline model at and above the thermocline depth as long as anisotropic covariances computed from the remote sensing data are used. Below the thermocline, the two merging techniques give similar performance.

1. Introduction

Observation networks combining in situ platforms and remote sensing are envisioned to increase the spatiotemporal coverage of measurements [e.g., the U.S. Integrated Ocean Observing System (IOOS) or the Australian Integrated Marine Observing System (IMOS)]. Because of their autonomy, motion controllability, and endurance at sea, gliders have led to significant improvements in networking capabilities to sample marine environments. Gliders are autonomous underwater platforms that use buoyancy changes to move between the surface and the ocean interior with a net horizontal displacement (Eriksen et al. 2001; Sherman et al. 2001; Webb et al. 2001). Operating these platforms in small fleets can greatly improve the monitoring of ocean regions (Ramp et al. 2009; Leonard et al. 2010).

While remote sensing regularly samples some surface ocean properties over vast areas, gliders are now mature enough to provide sustained in situ observations of the ocean interior. Thus, exploitation of synergism between observations from a glider fleet and remote sensing is becoming relevant. Some studies have investigated the complementarity between observations from a single glider and remote sensing. Montes-Hugo et al. (2009) analyzed the feasibility to complement glider and remote sensing observations to estimate the spatial distribution of inherent optical properties (IOPs) in the Antarctic Peninsula. Temperature and salinity profiles from a glider operating in the Balearic Sea were used by Bouffard et al. (2010) to improve along-track satellite altimetry. Methodologically, a functional optimal interpolation technique merging glider-like profiles and sea surface temperature (SST) was investigated by Alvarez and Reyes (2010) to infer 3D underwater thermal fields in an area off the Bosphorus Strait. This approach, which is adapted to the continuous distribution of glider measurements and exploits a 3D covariance function directly built from the present satellite information and the glider profiles, was found by the authors to be slightly superior to the discrete optimal interpolation. Alternatively, Alvarez (2011) used thin-plate splines to merge SST satellite imagery with temperature samples from an autonomous underwater vehicle (AUV) in a small (a few square kilometers) coastal region in the Baltic Sea, with the aim to obtain the most likely 3D ocean thermal distribution compatible with AUV observations and the surface boundary conditions imposed by the remotely sensed SST.

A field experiment (REP10) was carried out by the North Atlantic Treaty Organization (NATO) Undersea Research Centre (NURC) in the western Mediterranean Sea in 2010 to investigate the performance of a fleet of gliders supported by remote sensing data to characterize a marine coastal area. The objective of the present study is to exploit the glider, satellite, and in situ validation dataset collected during REP10 experiment

Corresponding author address: A. Alvarez, NATO Undersea Research Center, Viale San Bartolomeo 400, 19126 La Spezia, Italy.
E-mail: alvarez@nurc.nato.int

DOI: 10.1175/JTECH-D-12-00015.1

to compare the two above-mentioned merging procedures. Section 2 summarizes the two mathematical procedures. The field experiment is described in section 3. Results are reported in section 4. Finally, section 5 discusses and concludes the work.

2. Field estimations: Merging remote sensing and glider fleet observations

a. Functional optimal interpolation

The merging approach proposed by Alvarez and Reyes (2010) is first considered to estimate the volumetric thermal field in the REP10 area. A scalar oceanographic field $\psi(\mathbf{x})$ is assumed to be densely sampled by a fleet of M gliders along M tracks $\Gamma = \{\cup\Gamma_j\}_{j=1,\ldots,M}$ in a marine region Ω. Measurements are considered synoptic, so that no time dependence is considered. This assumption is typically valid for oceanic mesoscale variability and time periods of several days. The scalar field is hypothesized to be statistically described by a weakly stationary or second-order stationary process defined by a spatially constant mean $\overline{\psi}$ and a given covariance function $\mathrm{cov}(\mathbf{x}, \mathbf{x}')$. Field estimates at unobserved locations $\hat{\psi}(\mathbf{x})$ $(\mathbf{x} \in \Omega)$ are obtained with a functional linear response model:

$$\hat{\psi}(\mathbf{x}) = \overline{\psi} + \int_{\Gamma} \lambda(\mathbf{x}')[\psi(\mathbf{x}') - \overline{\psi}]\, d\mathbf{x}' \quad \mathbf{x} \in \Omega, \tag{1}$$

where $\lambda: \mathbf{x} \in \Gamma \rightarrow R$ is the weighting function for along-track observations. The weighting function $\lambda(\mathbf{x})$ $(\mathbf{x} \in \Gamma)$ minimizes the mean square error of the estimation when it verifies the linear system of integral equations:

$$\int_{\Gamma} \lambda(\mathbf{x}'')\, \mathrm{cov}(\mathbf{x}'', \mathbf{x}')\, d\mathbf{x}'' = \mathrm{cov}(\mathbf{x}', \mathbf{x}), \quad \text{with}$$
$$\mathbf{x}'', \mathbf{x}' \in \Gamma \text{ and } \mathbf{x} \in \Omega, \tag{2}$$

where $\mathbf{x}'$ and $\mathbf{x}''$ are points along Γ. Equation (2), which involves Fredholm integral equations of the first kind, describes an ill-posed problem generally associated with an unstable solution. Regularization methods are needed to approximate the true solution of Eq. (2). The solution is here approximated by a smooth function $\lambda'(\mathbf{x})$, $(\mathbf{x} \in \Gamma)$ resulting from the minimization of the following functional:

$$E(\beta) = \left\| \int_{\Gamma} \beta(\mathbf{x}'') C(\mathbf{x}', \mathbf{x}'')\, d\mathbf{x}'' - C(\mathbf{x}', \mathbf{x}) \right\|^2_{L_2} + \gamma \left\| \beta(\mathbf{x}) \right\|^2_{L_2}$$
$$\mathbf{x}'', \mathbf{x}' \in \Gamma \text{ and } \mathbf{x} \in \Omega, \tag{3}$$

where subscript L_2 indicates the L_2 norm ($\|f(x)\|_{L_2} = \{\int [f(x)]^2\, dx\}^{1/2}$) and γ is a nonnegative regularization parameter estimated from data using the discrepancy principle (Hansen 1998). This merging method requires a covariance matrix representative of the 3D spatial variability of the oceanographic field. The estimation of the covariance matrix over the study area is described in section 4.

b. Spline models

Alternatively, the merging method proposed by Alvarez (2011) is used to estimate the ocean temperature field. The volumetric estimation of the scalar oceanographic field $\psi(\mathbf{x})$ is determined as the most probable 3D field distribution compatible with observations and certain smoothness constraints. The conditional probability distribution of the field $\psi(\mathbf{x})$ given a set of observations $\{d(x_i, y_i, z_i)\}_{i=1,\ldots,N}$ with sampling uncertainties $\{\sigma_i\}_{i=1,\ldots,N}$ is

$$P(\psi \mid \{d_i\}_{i=1,\ldots,N}) \propto e^{-\sum_{i=1}^{N} \frac{[\psi(\mathbf{x}_i) - d_i]^2}{2\sigma_i^2} - F(\psi)}. \tag{4}$$

The first term in the exponential corresponds to the maximum likelihood density, while the second term refers to the a priori probability density determined by field smoothness assumptions. The maximum a posteriori (MAP) estimate verifies

$$\hat{\psi}^{\mathrm{MAP}}(\mathbf{x}) = \arg\min_{\psi} \left\{ \sum_{i=1}^{N} \frac{[\psi(\mathbf{x}_i) - d_i]^2}{2\sigma_i^2} + F(\psi) \right\}. \tag{5}$$

The so-called membrane models $F(\psi) \propto \int\int\int_{\Omega} |\nabla\psi|^2\, dx\, dy\, dz$ and thin-plate models $F(\psi) \propto \int\int\int_{\Omega} |\nabla^2\psi|^2\, dx\, dy\, dz$ are commonly employed in Eq. (5) to impose smoothness constraints. Here, the smoothness constraint is represented by the functional form $F(\psi) = \gamma_1 \int\int\int_{\Omega} |\nabla\psi|^2\, dx\, dy\, dz + \gamma_2 \int\int\int_{\Omega} |\nabla^2\psi|^2\, dx\, dy\, dz$, where γ_1 and γ_2 are weighting factors determined from the measurements[1] (Wahba 1990). The first term is supposed to suppress unnatural oscillations in the solution, while the second one ensures its differentiability. Note that $\hat{\psi}^{\mathrm{MAP}}(\mathbf{x})$ satisfies the Euler–Lagrange equation associated with Eq. (5), which involves harmonic and biharmonic operators (Inoue, 1986). The merging of glider fleet observations and remote sensing is obtained by solving Eq. (5) with a variational approach where satellite data fix Dirichlet boundary conditions at the sea surface

[1] Note that $\gamma_1 = 3.2 \times 10^{-4}\ ^{\circ}\mathrm{C}^{-2}\ \mathrm{m}^{-1}$ and $\gamma_2 = 3.6 \times 10^{-7}\ ^{\circ}\mathrm{C}^{-2}\ \mathrm{m}^{-1}$ with the present dataset.

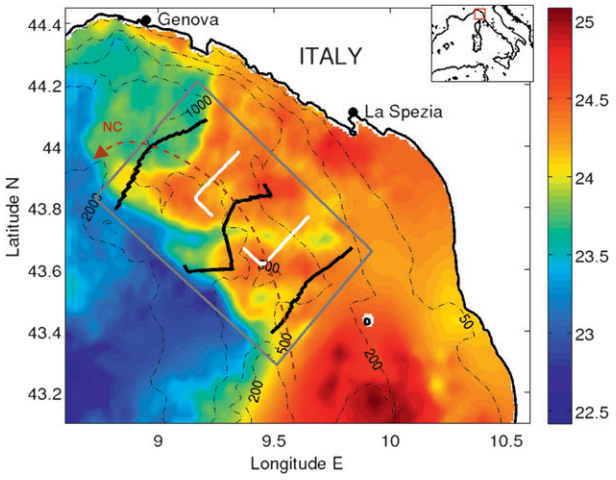

FIG. 1. REP-10 field experiment. The area delimited by the gray rectangle was monitored by three Slocum gliders (black lines) and remote sensing SST (colored field in °C) on 21 August. Validation data were collected by a towed ScanFish along the two white lines. Dashed black contours display the 50-, 200-, 500-, 1000-, and 2000-m isobaths. The average Northern Current path is illustrated by the dashed brown arrow.

$\psi(x, y, 0)$ [see Alvarez (2011) for details of the numerical implementation].

3. REP10 field experiment

The REP10 field experiment was conducted by the NATO Undersea Research Center in an area offshore La Spezia, Italy, in the Ligurian Sea (western Mediterranean) from 20 August to 3 September 2010. In particular, a nearly rectangular area of approximately 60 km × 90 km was sampled by three gliders and the NATO research vessel (NRV) *Alliance* from 20 to 22 August (see Fig. 1). Depth values range from 50 m to almost 1800 m in this region. The area is oceanographically characterized by an along-slope frontal system that separates lighter and warmer coastal waters from denser and colder waters of the central Ligurian Sea (Astraldi and Gasparini 1992). The main stream associated to the front, the Northern Current (NC; see Fig. 1), flows along the continental slope with speeds of 0.3–0.4 m s^{-1} up to approximately 200-m depth.

A fleet of three Slocum coastal gliders was deployed on 20 August at the westernmost boundary of the selected region. Deployments were equidistant, with two gliders at the northern and southern boundaries and the last one on the centerline of the region. The platforms transited the region until 22 August following roughly straight cross-shore trajectories. A total of 419 ''vertical'' profiles of water temperature were collected by the fleet between 20- and 180-m depth with a horizontal interval of approximately 400 m using an unpumped Seabird 41 CTD with an accuracy of 0.002°C and a resolution of 0.001°C. The 1-km resolution ultra-high Mediterranean resolution sea surface temperature analysis obtained on 21 August (Fig. 1) is used as surface temperature information from remote sensing. This product combines infrared measurements collected from various satellites through a statistical interpolation (B. Buongiorno-Nardelli 2010, personal communication).

To validate estimates, a towed ScanFish MK II vehicle equipped with a SeaBird 49 CTD was employed to sample the ocean temperature with a 500-m horizontal resolution. The temperature resolution of the sensor is 0.0001°C with an accuracy of 0.002°C. This platform followed an L-shaped trajectory with minor and major legs with lengths of 2 and 15 km, respectively, on both sides of the centerline of the region. The towed vehicle undulated between 3 and 70 m, with horizontal and vertical speeds of 3 and 1 m s^{-1}, respectively.

4. Results

a. Anisotropic covariance

Separate horizontal and vertical covariances were used to build a 3D covariance model. The horizontal covariance was computed assuming SST observations as realizations of a Gaussian, weakly stationary, and anisotropic random process, that is, a Gaussian random field with a spatially constant mean and translational invariance in along- and cross-shore directions: $\mathrm{cov}_H[T(\mathbf{x}), T(\mathbf{y})] = F(|\varsigma_\mathbf{x} - \varsigma_\mathbf{y}|, |\eta_\mathbf{x} - \eta_\mathbf{y}|)$, ς and η being the point coordinates, $T(\mathbf{x})$ the temperature field and $F(.)$ a function determined from SST imagery. Vertical covariance was deduced from the observations collected by the gliders. Specifically, thermal fluctuations around a mean vertical profile were characterized by a vertical covariance $\mathrm{cov}_V[T(\mathbf{x}), T(\mathbf{y})] = G(|z_\mathbf{x} - z_\mathbf{y}|)$, where z is the vertical point coordinate and $G(.)$ a function determined from the observations. Horizontal and vertical covariances were then combined through a tensor product to provide the 3D covariance $\mathrm{cov}_{3D}[T(\mathbf{x}), T(\mathbf{y})] = F(|\varsigma_\mathbf{x} - \varsigma_\mathbf{y}|, |\eta_\mathbf{x} - \eta_\mathbf{y}|) \otimes G(|z_\mathbf{x} - z_\mathbf{y}|)$. Following Alvarez and Reyes (2010), covariance values at required spatial lags were obtained from interpolating the gridded numerical covariance. Figures 2a and 2b display the resulting horizontal and vertical covariance. The anisotropic covariance is characterized by a larger decorrelation scale (defined by the *e*-folding distance) in the northward (13 km) than in the westward (8 km) direction (Fig. 2a). Along the vertical (Fig. 2b), notice that the decorrelation length is about 8 m, indicating limited vertical correlations in the collected temperature profiles.

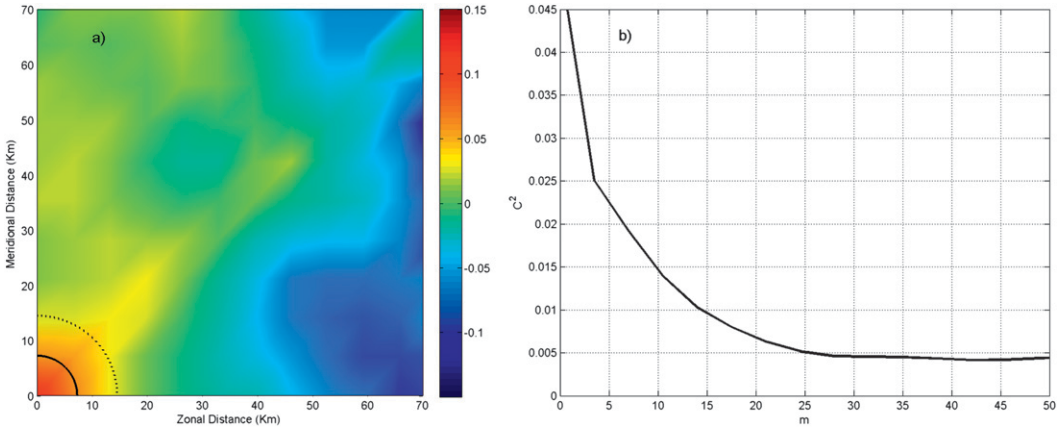

FIG. 2. (a) Anisotropic horizontal covariance (color scale in $°C^2$) and contours of the isotropic horizontal covariance matrix (solid and dotted lines correspond to the 0.07° and 0.035°C^2 contours, respectively) computed from SST imagery and (b) vertical covariance inferred from gliders observations.

b. Validation

The volumetric reconstructions resulting from both estimation procedures are displayed in Fig. 3 as superposition of isothermal surfaces. Qualitatively, the optimal interpolation estimate is characterized by higher temperatures in the surfacemost layer and a more pronounced eastward deepening of the thermocline compared to the spline estimate. The differences between temperature estimates and observational values along the ScanFish track are illustrated in Fig. 4. The functional optimal interpolation approach results in accurate estimates (absolute error lower than 0.5°C), except in the layer between 20- to 30-m depth, where the thermocline is located (errors up to 3°C). The statistical approach underestimates the temperature field just above the thermocline, while it overestimates the thermal field in the thermocline. Estimate errors substantially decrease below the thermocline. Notice, however, that the covariance model is not expected to be valid below the thermocline, which thermally decouples the upper layer from the ocean interior. The good performance of the method in the deeper layer is associated with the small thermal variability below the thermocline. The overall root-mean-square error (RMSE) is 0.72°C with this approach. Concerning the spline model estimate, significant errors are spread between 10- and 35-m depth, being less correlated with the thermocline depth than in the previous case. Similarly to the functional interpolation approach, errors rapidly decrease below 35-m depth. The overall corresponding RMSE is 1.02°C.

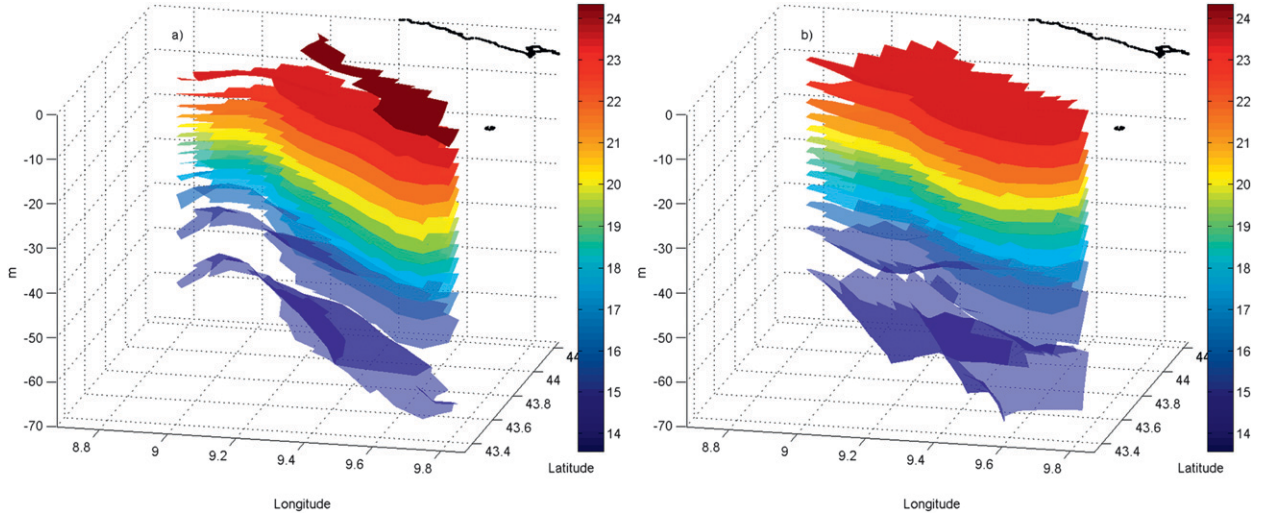

FIG. 3. Thermal field estimates obtained from the (a) anisotropic functional optimal interpolation and (b) spline models. Color scale is in degrees Celsius.

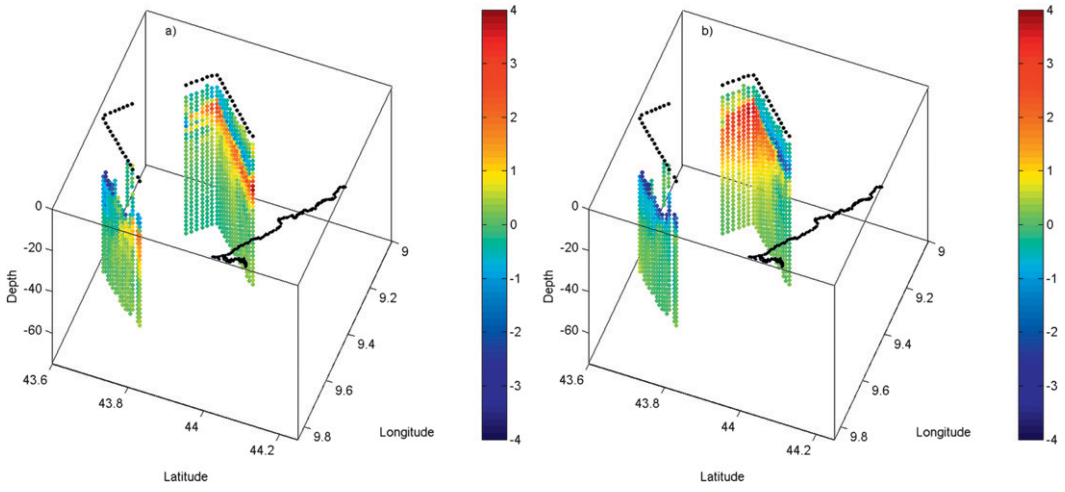

FIG. 4. Estimate errors at validation locations for the (a) anisotropic functional optimal interpolation and (b) spline models. Color scale is in degrees Celsius. The black line represents the coastline, while the black dots illustrate the surface projection of the ScanFish observations.

The vertical distributions of the estimation error for both merging methodologies are compared in Fig. 5. The RMSE profile was computed by segmenting the error profiles into layers of 8-m thickness. The estimation error obtained with a functional optimal interpolation using an isotropic 3D covariance model deduced from the SST data is also displayed for comparison. The isotropic horizontal covariance has an amplitude of $0.1°C^2$ and a horizontal decorrelation length of 11 km. The overall RMSE is 0.78°C for this third model. The vertical distributions of the RMSE associated with the climatological (MED6 climatology; Brankart and Pinardi 2001) and the average glider profile are also shown in the figure (corresponding overall RMSEs are 1.43° and 0.97°C, respectively).

Both functional optimal interpolation approaches perform substantially better than the rest of the models at estimating temperatures at the thermocline depth. The anisotropic and spline models outperform the isotropic model between the surface and 10-m depth, which demonstrates the positive impact on the temperature estimate of the remote sensing information, whether included as anisotropic covariances or boundary conditions on the temperature estimate. When considering the whole surface layer above the thermocline (0- to 20-m depth), the best temperature estimate is obtained from the anisotropic functional model. Around the thermocline depth (20- to 30-m depth), isotropic and anisotropic functional models provide similar RMSE values between 0.97° and 1.35°C, while the spline model RMSE ranges from 1.50° to 2.15°C. No significant difference is found below the thermocline among the different estimation models.

Notice that the spline model does not provide here any improvement with respect to the average glider profile.

5. Discussion

The performance of different methodologies to merge SST remote sensing and in situ observations obtained from a fleet of three gliders was investigated in this article. An optimal interpolation generalized to functional-like datasets was first considered to merge data from

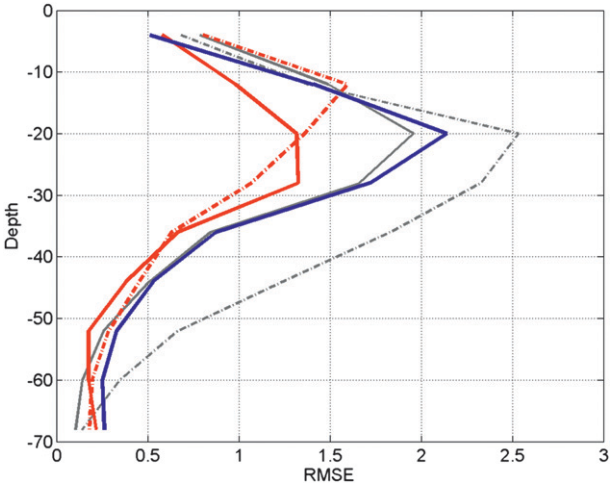

FIG. 5. Vertical distribution of the RMSE for the anisotropic (red solid line) and isotropic (red dashed-dotted line) functional optimal interpolation, spline model (blue line), average profile model (solid gray line), and climatological profile model (dashed-dotted gray line).

remote sensing and glider fleets. A second procedure based on spline models was then implemented for the same purpose. Field estimates were confronted to independent temperature measurements collected by a towed ScanFish vehicle along predetermined validation tracks.

The best overall performance was obtained by the anisotropic functional optimal interpolation model, with a nonuniform distribution of the estimation error along the vertical. In the surface layer above the thermocline, the anisotropic functional model outperforms its isotropic counterpart and the spline model. This results from the better representation of the regional spatial variability provided by the anisotropic covariance compared to the isotropic covariance or the smoothness constraints. The performance of the different models progressively deteriorates along the vertical down to the thermocline depth. The performance loss with depth is more pronounced for the spline model than for the anisotropic optimal interpolation. The spline model is not found to improve the estimate provided by the average glider profile over the whole area. This could be a consequence of the smoothing impact of the harmonic and biharmonic operators underlying the spline technique. Besides, it is reasonable to assume that the anisotropic covariance model inferred from remote sensing remains valid down to the thermocline depth. At this depth, isotropic and anisotropic models show similar RMSE values. Below the thermocline, the use of anisotropic surface properties does not significantly improve the temperature estimate. All models provide similar performance below the thermocline where the spatial variability is small.

To conclude, this study recommends the functional optimal interpolation based on surface anisotropic covariance as the best procedure to estimate the ocean temperature field from observations gathered by remote sensing and a glider fleet in the surfacemost layer. Below the thermocline, information obtained from remote sensing loses validity and procedures based on a background field and covariances taken from historical databases may efficiently complement this technique that exclusively integrates information from present observations.

REFERENCES

Alvarez, A., 2011: Volumetric reconstruction of oceanographic fields estimated from remote sensing and in situ observations from autonomous underwater vehicles of opportunity. *IEEE J. Oceanic Eng.,* **36,** 12–24.

——, and E. Reyes, 2010: Volumetric estimation of thermal fields inferred from glider-like and remote-sensing measurements in undersampled coastal regions. *J. Geophys. Res.,* **115,** C11006, doi:10.1029/2009JC005791.

Astraldi, M., and G. P. Gasparini, 1992: The seasonal characteristics of the circulation in the north Mediterranean basin and their relationship with the atmospheric-climatic conditions. *J. Geophys. Res.,* **97** (C6), 9531–9540.

Bouffard, J., A. Pascual, S. Ruiz, Y. Faugère, and J. Tintoré, 2010: Coastal and mesoscale dynamics characterization using altimetry and gliders: A case study in the Balearic Sea. *J. Geophys. Res.,* **115,** C10029, doi:10.1029/2009JC006087.

Brankart, J. M., and N. Pinardi, 2001: Abrupt cooling of the Mediterranean Levantine Intermediate Water at the beginning of the eighties: Observational evidence and model simulation. *J. Phys. Oceanogr.,* **31,** 2307–2320.

Eriksen, C. C., T. J. Osse, R. D. Light, T. Wen, T. W. Lehman, P. L. Sabin, J. W. Ballard, and A. M. Chiodi, 2001: Seaglider: A long-range autonomous underwater vehicle for oceanographic research. *IEEE J. Oceanic Eng.,* **26,** 424–436.

Hansen, P. C., 1998: *Rank-Deficient and Discrete Ill-Posed Problems: Numerical Aspects of Linear Inversion.* SIAM, 247 pp.

Inoue, H., 1986: A least-squares smooth fitting for irregularly spaced data: Finite-element approach using the cubic B-spline basis. *Geophysics,* **51,** 2051–2066.

Leonard, N., D. Paley, R. Davis, D. Fratantoni, F. Lekien, and F. Zhang, 2010: Coordinated control of an underwater glider fleet in an adaptive ocean sampling field experiment in Monterey Bay. *J. Field Robot.,* **27,** 718–740.

Montes-Hugo, M. A., R. Gould, R. Arnone, H. Ducklow, K. Carder, D. English, O. Schofield, and J. Kerfoot, 2009: Beyond the first optical depth: Fusing optical data from ocean color imagery and gliders. *Ocean Remote Sensing: Methods and Applications,* R. J. Frouin, Ed., International Society for Optical Engineering (SPIE Proceedings, Vol. 7459), doi:10.1117/12.828851.

Ramp, S., and Coauthors, 2009: Preparing to predict: The second autonomous ocean sampling network (AOSN-II) experiment in the Monterey Bay. *Deep-Sea Res. II,* **56,** 68–86.

Sherman, J., R. E. Davis, W. B. Owens, and J. Valdes, 2001: The autonomous underwater glider ''Spray.'' *IEEE J. Oceanic Eng.,* **26,** 437–446.

Wahba, G., 1990: *Spline Models for Observational Data.* SIAM, 165 pp.

Webb, D. C., P. J. Simonetti, and C. P. Jones, 2001: SLOCUM: An underwater glider propelled by environmental energy. *IEEE J. Oceanic Eng.,* **26,** 447–452.

Document Data Sheet

Security Classification		Project No.
Document Serial No.	**Date of Issue**	**Total Pages**
CMRE-PR-2014-002	January 2014	6 pp.

Author(s)

Alvarez, A., Mourre, B.

Title

Oceanographic field estimates from remote sensing and glider fleet.

Abstract

This work investigates the merging of temperature observations from a glider fleet and remote sensing, based on a field experiment conducted in an extended coastal region offshore La Spezia, Italy, in August 2010. Functional optimal interpolation and spline formalisms are used to integrate temperature profiles from a fleet of three gliders with remotely sensed sea surface temperature into a volumetric thermal field estimate. Independent measurements from a towed ScanFish vehicle are used for validation. Results indicate that the optimal interpolation approach performs better than the spline model at and above the thermocline depth as long as anisotropic covariances computed from the remote sensing data are used. Below the thermocline, the two merging techniques give similar performance.

Keywords

Issuing Organization

Science and Technology Organization
Centre for Maritime Research and Experimentation

Viale San Bartolomeo 400, 19126 La Spezia, Italy

[From N. America:
STO CMRE
Unit 31318, Box 19, APO AE 09613-1318]

Tel: +39 0187 527 361
Fax:+39 0187 527 700

E-mail: library@cmre.nato.int